Rossby Wave–Coastal Kelvin Wave Interaction in the Extratropics. Part II: Formation of Island Circulation

ZHENGYU LIU AND LIXIN WU

Department of Atmospheric and Oceanic Sciences, University of Wisconsin—Madison, Madison, Wisconsin

H. HURLBURT

Navy Research Laboratory, Stennis Space Center, Bay St. Louis, Mississippi

(Manuscript received 13 May 1998, in final form 1 September 1998)

ABSTRACT

The formation of an island circulation is investigated both theoretically and numerically in light of the dynamics of coastal Kelvin waves and Rossby waves. An island circulation is formed in three stages. First, the direction of the circulation is initiated by the coastal Kelvin wave; second, the transport of the circulation is established by the short Rossby wave dissipated against the eastern coast of the island; and finally, the basinwide circulation pattern is completed by the long Rossby wave radiated from the western coast of the island. An island circulation can be forced by either a local alongshore wind or a remote vorticity forcing to the east of the island; the initial Kelvin wave is directly forced by the alongshore wind in the former case, but indirectly forced by a planetary wave incident on the eastern coast of the island in the latter case. A comparison is also made between the spinup of an island circulation and a basin circulation. In addition, this spinup study also provides an alternative derivation of the island rule in light of the dynamics of Kelvin and Rossby waves. The implication for understanding the temporal response of an island circulation to a variable forcing is also discussed.

1. Introduction

In an ocean basin that contains an island, the total circulation transport around the island is determined by the large-scale wind forcing according to the ''Island Rule'' (Godfrey 1989). The island rule has been extended and applied to the Indonesian Throughflow (Godfrey 1989; Wajsowicz 1993a,b, 1996; Hirst and Godfrey 1993; Masumoto and Yamagata 1996) and North Hawaiian Ridge Current (Qiu et al. 1997; Qiu et al. 1999). The island rule has also been thoroughly examined and further developed in theory as well as with laboratory and numerical experiments (Wajsowicz 1993a; Pedlosky et al. 1997; Qiu et al. 1999; Pedlosky and Spall 1999). Following Godfrey (1989), all these works have derived the island rule by integrating the momentum equation along a closed route that avoids the eastern coast of the island and in turn avoids the complex dynamics of the western boundary currents.

The present work will investigate the formation of an island circulation with the focus on the dynamic role of the coastal Kelvin wave and Rossby wave. It will be shown that the island circulation can be generated by either a local alongshore wind stress or a remote vorticity forcing to the east of the island. In either case, the wave dynamics will be shown to be essential in the formation of the island circulation. The study of wave dynamics also provides an alternative approach to the derivation of the island rule. During the spinup of an island circulation, first, the direction of the island circulation is set up by the coastal Kelvin wave. This Kelvin wave can be forced by coastal upwelling in the case of local wind forcing or forced by incident long Rossby waves in the case of remote forcing. The Kelvin wave also generates short and long Rossby waves on the eastern and western coasts of the island, respectively. The strong damping of the short Rossby wave balances the forcing and enables the transport of the island circulation to reach its equilibrium. Finally, the basinwide pattern associated with the island circulation is completed after the propagation of the long Rossby wave that is generated on the western coast of the island.

The paper is arranged as follows. Section 2 presents a simple theory on the formation of an island circulation forced by a local alongshore wind. This study also provides an alternative derivation of the island rule in light of Kelvin and Rossby waves. The theory is substantiated by numerical experiments in section 3. Section 4 further

Corresponding author address: Z. Liu, Department of Atmospheric and Oceanic Sciences, University of Wisconsin—Madison, 1225 W. Dayton St., Madison, WI 53706-1695.
E-mail: znl@ocean.meteor.wisc.edu

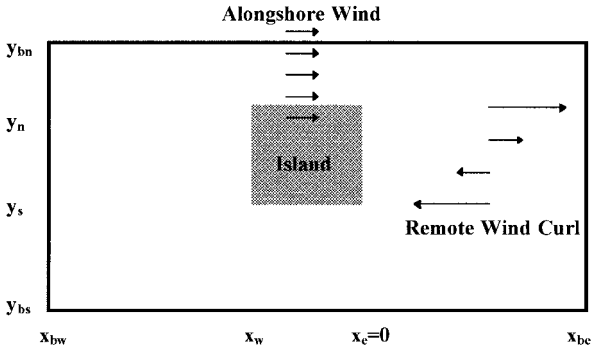

FIG. 1. Schematic figure for the setup of the island circulation in a basin. A local alongshore wind and a remote wind curl to the east of the island are also shown.

studies the island circulation forced by a remote forcing to the east of the island. A summary and further discussion are given in section 5.

2. Island circulation forced by local wind: The theory

According to the island rule, the transport to the east of an island (located for our example in the Northern Hemisphere as in Fig. 1) is contributed by two parts:

$$T_I \equiv D \int_{X_e}^{X_{be}} v\, dx = T_{\text{local}} + T_{\text{remote}}. \qquad (2.1a)$$

The first part is locally forced by the wind stress around the island, $\Gamma_\tau \equiv \oint_{\text{island}} \boldsymbol{\tau} \cdot d\boldsymbol{l}/\rho D$, as

$$T_{\text{local}} = \frac{D\Gamma_\tau}{f_n - f_s}. \qquad (2.1b)$$

The second part is a remote contribution that equals the meridionally averaged Sverdrup transport as

$$T_{\text{remote}} = \frac{\int_{y_s}^{y_n} T_{\text{Sv}}(y)\, dy}{y_n - y_s}, \qquad (2.1c)$$

where $T_{\text{Sv}}(y)$ is the transport of the Sverdrup flow to the east of the island at latitude y. Here D is the mean depth of the upper layer of our 1.5-layer ocean; f_n and f_s are the Coriolis parameters at the northern and southern tips of the island, respectively. The remotely forced island transport (2.1c) also applies to the circulation around a deep ocean ridge forced by a mass entrainment (Pedlosky 1994; Pedlosky et al. 1997).

In this section, we will focus on the effect of a local alongshore wind stress forcing. It is instructive to first have a qualitative discussion on how an island circulation is spun up by an alongshore wind in the upper ocean. The discussion will be substantiated later both analytically and numerically. For simplicity, the island and basin are assumed to be rectangular, and the local wind forcing is a patch of nearly uniform eastward wind stress to the north of the island (Fig. 1). The onset of an eastward wind north of the island generates a southward surface Ekman drift, which then produces a coastal downwelling along the northern coast of the island. The downwelling forces a Kelvin wave with a positive sea surface height (SSH) (or thermocline depth). The Kelvin wave circles around the island in a short time of $t_{\text{island}\,K} = L_{\text{island}}/C_K$, where L_{island} is the circumference of the island and C_K is the Kelvin wave speed. This establishes a coastal Kelvin wave current that flows in a clockwise direction and is trapped within about a deformation radius of the coast (Fig. 2a). This completes the first stage of the island circulation formation, with the direction of the circulation being set up by the coastal Kelvin wave. The transport of the island circulation, however, is still increasing because of the input of the persistent angular momentum of the wind. In the meantime, the Kelvin wave current extracts (sheds) mass along the eastern (western) coast of the island to generate short (long) Rossby waves because of the increased (decreased) deformation radius with latitude (Miles 1972; Godfrey 1975).

To the east of the island, short Rossby waves are trapped by dissipation against the coast, forming a narrow southward western boundary current (Pedlosky 1965). This narrow boundary current effectively damps the energy input from the wind and limits the circulation to an equilibrium transport within a damping timescale t_{damp} (Fig. 2b). This leads to the completion of the second stage of the circulation formation in which the transport of the island circulation is determined by the short Rossby wave.

Although the transport has reached equilibrium, the pattern of the island circulation still evolves west of the island because of the propagation of the long Rossby wave that is generated along the western coast of the island. The long wave carries with it the northward transport of the Kelvin wave current that is initiated on the western coast of the island (Fig. 2c). After the long wave crosses the basin, the northward current is arrested by short Rossby waves on the western boundary of the basin. A steady island circulation pattern is finally achieved. This is the final stage of the island circulation formation. This hypothetical experiment suggests that the equilibrium island transport can be estimated from the wave dynamics of the Kelvin wave and damped short Rossby waves at the eastern coast of the island. In the following, we further show that the transport estimated from the wave dynamics is the same as that derived from the island rule.

We will study the island circulation in a 1.5-layer fluid model on a beta plane $f = f_0 + \beta y$, where f_0 is the mean Coriolis parameter of the island. The circulation is forced by a local wind stress patch north of the island as shown in Figs. 1 and 2. In this case, the transport of the island circulation in (2.1) is forced by the first term only because of the absence of a Sverdrup

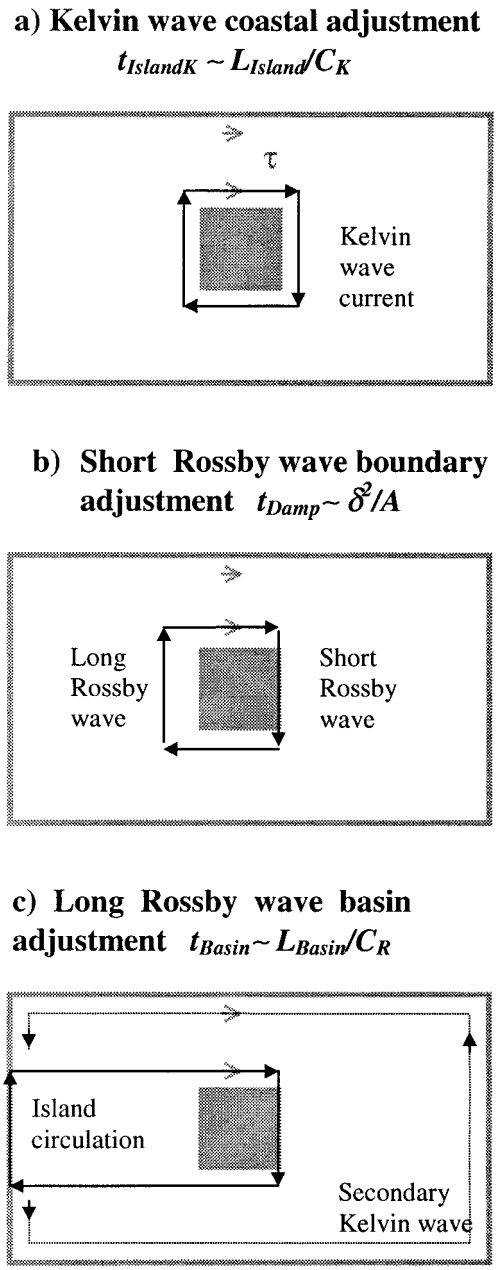

FIG. 2. Schematic figures for the formation of an island circulation forced by a local alongshore wind stress forcing (gray arrows north of the island). (a) Initial stage in which the direction of the island circulation is initiated by the adjustment of the primary Kelvin wave coastal current around the island. (b) The second stage in which the equilibrium island transport (1) is achieved; the alongshore wind stress forcing is balanced by the short Rossby waves damped against the eastern coast of the island. (c) The final stage in which the spatial pattern of the island circulation is completed by the long Rossby wave, which is generated by the Kelvin wave on the western coast of the island and which propagates westward and is finally arrested by the western boundary of the basin. This long wave also generates a secondary Kelvin wave current on the basin boundary (the arrow dashed lines). In all figures, the island circulation is plotted in dark solid lines with arrows.

flow to the east of the island. With standard notations, the linear 1.5-layer model is

$$\partial_t u - fv = -g\partial_x h + \tau^x/\rho D + A\nabla^2 u \quad (2.2a)$$

$$\partial_t v + fu = -g\partial_y h + \tau^y/\rho D + A\nabla^2 v \quad (2.2b)$$

$$\partial_t h + H(\partial_x u + \partial_y v) = 0, \quad (2.2c)$$

where a Laplace momentum mixing has been included; the perturbation SSH is h, and the equivalent depth is $H = D\Delta\rho/\rho$. The circulation integral around the island can be obtained by integrating (2.2a,b) around the island clockwise as (Wajsowicz 1993a; Pedlosky et al. 1997)

$$\partial_t \oint_{\text{island}} \mathbf{u} \cdot dl = \Gamma_\tau + A \oint_{\text{island}} \nabla^2 \mathbf{u} \cdot dl. \quad (2.3)$$

We will focus on the baroclinic flow because it has well-separated timescales of adjustment. However, it should be kept in mind that virtually all the discussions here can be applied equally to a shallow water, flat-bottom barotropic fluid after the equivalent depth H is replaced by the total depth D.

Now we study the circulation in terms of Kelvin and Rossby waves. Following McCalpin (1995), we break the total wave field into the Kelvin wave and Rossby wave parts: $u = u_K + u_R$, $v = v_K + v_R$, $h = h_K + h_R$. The equations for a coastal Kelvin wave with a reference latitude f_c are

$$\partial_t u_K - f_c v_K = -g\partial_x h_K + A\nabla^2 u_K \quad (2.4a)$$

$$\partial_t v_K + f_c u_K = -g\partial_y h_K + A\nabla^2 v_K \quad (2.4b)$$

$$\partial_t h_K + H(\partial_x u_K + \partial_y v_K) = 0. \quad (2.4c)$$

Notice that f_c could vary from face to face for a rectangular island such as that in Fig. 1. At the low frequency limit, the Kelvin wave along the island can be approximated as an alongshore geostrophic current with a uniform coastal SSH (see section 3).[1] Indeed, since the Kelvin wave speed $C_K = (gH)^{1/2}$ is independent of forcing frequency, the Kelvin wave has an alongshore wavelength approaching infinity for a zero frequency forcing. Thus, this coastal Kelvin wave current around the island is approximately

$$h_K = K(t)(e^{-(y-y_n)/r_N} + e^{-x/r_o} + e^{(y-y_s)/y_s} + e^{(x-x_w)/r_o}), \quad (2.5)$$

where $r_c = C_K/f_c$ is the deformation radius at f_c. The first, second, third, and fourth terms on the right-hand side of (2.5) represent the Kelvin wave on the northern, eastern, southern, and western coasts of the island, respectively. Because the Kelvin wave propagates rapidly and has a fixed spatial structure, it should not be affected much by

[1] The amplitude of the Kelvin wave varies with the Coriolis parameter as $f^{1/2}$, because of energy conservation (Miles 1972). In the middle latitude, this change is usually about 10%–20% within a latitude extension of 10°–20°.

dissipation. The first stage is the Kelvin wave coastal adjustment stage, which lasts till about $t_{\text{island }K} = L_{\text{island}}/C_K$. In this stage, the Kelvin wave travels around the island, building a coastal current. After this stage, but before the second stage when the dissipation of the short Rossby wave becomes important, the amplitude of the Kelvin wave current (2.5) can be derived from the circulation integral (2.3) as approximately

$$K(t) \approx t\Gamma_\tau (H/g)^{1/2}/L_{\text{island}}, \tag{2.6}$$

where the alongshore current is derived geostrophically from (2.5). The Kelvin wave amplitude, and in turn the alongshore geostrophic transport $T_I = -K(t)g/f_0$, increases linearly with time because of the lack of dissipation against the persistent wind forcing.

The Rossby wave component satisfies

$$\partial_t u_R - fv_R = -g\partial_x h_R + A\nabla^2 u_R + F_x \tag{2.7a}$$

$$\partial_t v_R + fu_R = -g\partial_y h_R + A\nabla^2 v_R + F_y \tag{2.7b}$$

$$\partial_t h_R + H(\partial_x u_R + \partial_y v_R) = 0. \tag{2.7c}$$

Here the forcings

$$F_x = (f - f_c)v_K + \tau^x/\rho D,$$

$$F_y = -(f - f_c)u_K + \tau^y/\rho D \tag{2.8}$$

include not only the wind stress but also the Kelvin wave. A generalized quasigeostrophic equation can be derived from (2.7) and (2.8) as (Anderson and Killworth 1979; Williams 1985; McCalpin 1995)

$$\partial_t h_R - \beta r^2 \partial_x h_R - r^2(\partial_t - A\nabla^2)\nabla^2 h_R + (2\beta r^2/f)(\partial_t - A\nabla^2)\partial_y h_R = -w_E + (H/f)[(f - f_c)(\partial_x u_K + \partial_y v_K) + (f_c/f)\beta v_K], \tag{2.9}$$

where w_E is the Ekman pumping velocity and $r = C_K/f$ is the deformation radius at f. For a uniform alongshore wind stress here, the Ekman pumping is approximately zero. Rossby waves are forced by the coastal Kelvin wave alone. Along the northern ($f_c - f_n = 0$) or southern ($f_c - f_s = 0$) coast, the Kelvin wave forcing vanishes because $v_K = \partial_y v_K = \partial_x u_K = 0$, and therefore no Rossby waves are generated according to Eq. (2.9). Along the eastern or western coast ($f_c \approx f_0$), the Kelvin wave has $u_K = 0$ and $\partial_y v_K = 0$. The forcing on the rhs of Eq. (2.9) is

$$(H/f)[(f_0/f)\beta v_K] = \beta r^2 \partial_x h_K, \tag{2.10}$$

where we have used $f_0 v_K = g\partial_x h_K$. Along the eastern coast, short Rossby waves are damped locally and reach a local equilibrium state in a short local vorticity damping time $t_{\text{damp}} = \delta^2/A$, which is on the order of 1 month for a Munk boundary layer width of about 10 km. This is much shorter than the basin scale adjustment time of the long Rossby wave $t_{\text{basin}} = L_{\text{basin}}/C_R$, where $C_R = \beta r^2$ is the speed of long Rossby waves. Thus, the local dynamics of the short Rossby wave are determined at the first order from Eq. (2.9) and (2.10) as

$$\partial_x h_R - \delta^3 \partial_{xxxx} h_R = -\partial_x h_K, \tag{2.11a}$$

where $\delta = (A/\beta)^{1/3}$ is the width of the Munk boundary layer (Pedlosky 1987), and

$$h_K = K(t)\exp(-x/r_0) \tag{2.11b}$$

is the Kelvin wave SSH along the eastern coast of the island according to Eq. (2.5). A similar discussion has been made by Godfrey (1975) in the case of an ocean basin. This is a forced Munk boundary layer problem. We will be most interested in the case of $\delta/r < 1$. Indeed, for a barotropic flow, the deformation radius r is at thousands of kilometers and therefore $\delta/r < 1$ is automatically satisfied. For a baroclinic flow, $\delta/r < 1$ requires that the dissipation is not too strong.

A free-slip boundary condition will be used at the coast ($x = 0$) as[2] $\partial_{xx} h = 0$. The homogeneous part of the h_R solution should also diminish toward the interior ($x/\delta \to \infty$). The condition of no normal flow at the coast is $\partial_y h_R = 0$, or $h_R = \text{const}$ at $x = 0$. Along the northern and southern boundaries $h_R = 0$, because no Rossby waves are generated. Thus, the continuity of pressure to the northern and southern boundaries of the island ensures that the no-normal flow condition becomes $h_R = 0$ at $x = 0$.

With the boundary conditions above, the damped short Rossby wave can be derived from (2.11) as

$$h_R = K(t)[M(x) - e^{-x/r_c}] + O[(\delta/r)^3], \tag{2.12}$$

where $M(x)$ satisfies $M - \delta^3 \partial_{xxx} M = 0$ and has the Munk boundary layer structure

$$M(x) = e^{-x/2\delta}\left[\cos\left(\frac{\sqrt{3}x}{2\delta}\right) - \frac{1}{\sqrt{3}}\sin\left(\frac{\sqrt{3}x}{2\delta}\right)\right]. \tag{2.13}$$

With (2.11b) and (2.12), the total SSH along the eastern coast of the island is, therefore,

$$h = h_K + h_R = K(t)M(x) + O[(\delta/r)^3]. \tag{2.14}$$

Indeed, the solution (2.14) becomes apparent if Eq. (2.11a) is rewritten as $(\partial_x - \delta^3\partial_{xxxx})(h_R + h_K) = \delta^3\partial_{xxxx}h_K$, and it is similar to the so-called Kelvin–Munk wave of Godfrey (1975) in a spindown study of ocean basin circulation. The total SSH has a spatial structure the same as the Munk boundary layer, but with an amplitude the same as that of the coastal Kelvin wave. Equivalently, the amplitude of the short Rossby wave (2.12) is the same as that of the coastal Kelvin wave $K(t)$ at the lowest order. This is the key result that will immediately lead to the island rule. Apparently, the

[2] The no-slip condition can be discussed similarly. In discussing the evolution of the circulation, the island integral in Eq. (2.3) should be considered as the average across the boundary layer. Bottom friction can also be discussed similarly in terms of the forced Stommel's boundary layer (Liu et al. 1999). Similarly, dissipation could modify the Kelvin wave solution (2.5) but will not change the conclusions at the leading order.

Kelvin wave coastal current (which has a width of r) is mainly canceled by the damped short Rossby wave except for the region within the Munk boundary layer.

Since the Munk boundary current is narrower than the deformation radius, the circulation around the island as well as the circulation's dissipation are produced mainly on the eastern coast of the island as

$$\oint_{\text{island}} \mathbf{u} \cdot d\mathbf{l} = \int_{y_s}^{y_n} v|_{x=0}\, dy + O(\delta/r) \approx -\frac{g(f_n - f_s)}{\delta\beta f_0} K(t) \tag{2.15a}$$

$$A \oint_{\text{island}} \nabla^2\mathbf{u} \cdot d\mathbf{l} = \int_{y_s}^{y_n} \partial_{xx} v|_{x=0}\, dy + O[(\delta/r)^3] \approx \frac{Ag(f_n - f_s)}{\delta^3\beta f_0} K(t) = \frac{g(f_n - f_s)}{f_0} K(t), \tag{2.15b}$$

where we have used $v = (g/f_0)\partial_x h$ and (2.14). In Eq. (2.15b), the net dissipation integral is independent of the dissipation coefficient A because the width of the Munk boundary layer (damped short Rossby wave) varies with A. A weaker (stronger) damping coefficient A is accompanied by a narrower (wider) boundary current, such that the net damping remains independent of the damping coefficient. This turns out to be the reason why the island transport is independent of damping, although the damped short Rossby wave plays the critical role in setting up the equilibrium island transport.

With (2.15a,b), the circulation integral (2.3) leads to the equation for amplitude evolution as

$$\frac{d}{dt}K(t) + \beta\delta K(t) = -\frac{\beta\delta f_0}{g(f_n - f_s)}\Gamma_\tau(t) \tag{2.16}$$

with the initial condition as $K(0) = 0$. After the spinup, Γ_τ is constant because the local wind remains unchanged with time. The amplitude K is therefore

$$K(t) = K_M(1 - e^{-t/t_{\text{damp}}}), \tag{2.17a}$$

where

$$K_M = \frac{-f_0}{g(f_n - f_s)}\Gamma_\tau, \qquad t_{\text{damp}} = \frac{1}{\delta\beta}. \tag{2.17b}$$

Therefore, the amplitude increases monotonically. After about t_{damp} the input wind stress is balanced by the dissipation of short Rossby waves on the eastern coast, resulting in an equilibrium island transport that corresponds to a maximum Kelvin wave amplitude K_M. The final geostrophic transport east of the island can be calculated as $T_I = -K_m g/f_0$, which gives a transport identical to that of the island rule (2.1b). It is now clear that the factor $f_n - f_s$ in the island rule arises from the dissipation of short Rossby waves along the eastern coast as seen in (2.15b). A longer latitude extent allows a longer dissipation boundary layer to damp the island circulation, and therefore leads to a smaller island transport. The time to reach an equilibrium transport t_{damp} is the time needed for the energy of the short Rossby wave to travel (at the group velocity $\beta\delta^2$) across the Munk boundary layer δ (Pedlosky 1965), which also equals the local vorticity damping time δ^2/A. For a Munk boundary layer width of about 10 km, t_{damp} is on the order of 1 month. This is the time required for the second stage of short Rossby wave boundary adjustment (Fig. 2b). In the next stage, the long Rossby wave generated on the western coast of the island propagates across the basin at the speed of $C_R = \beta r^2$; the total transport of the island circulation, however, remains unchanged. Finally, after the long wave reaches the western boundary of the basin at $t = (X_w - X_{bw})/C_R \sim t_{\text{basin}}$, a steady island circulation pattern is mostly completed (Fig. 2c).

It is interesting to compare the adjustment of an island circulation and a basin circulation. For the uniform eastward wind stress north of the island, an upwelling is also generated on the northern boundary of the basin. This upwelling forces a Kelvin wave of negative SSH. A clockwise Kelvin wave current around the basin boundary (Fig. 3a) is established similar to that around the island (Fig. 2a). This basin boundary Kelvin wave generates short Rossby waves against the western boundary of the basin (Fig. 3b), again similar to the short wave boundary adjustment in the island case (Fig. 2b). After this adjustment, the transport of the basin boundary current can also be determined by the island rule (2.1) [or (2.17b)], if one replaces $f_n - f_s$ with Coriolis parameter change across the latitude of the basin $f_{bn} - f_{bs}$. However, the final transport around the basin vanishes, in sharp contrast to the island case. This occurs because the long Rossby wave from the eastern boundary of the basin crosses the basin (Figs. 3b–d), carrying with it a current transport of the same magnitude, but in the opposite direction of the basin western boundary current. Therefore, the transport of the basin western boundary current is canceled exactly after the arrival of the basin eastern boundary Rossby wave. This is consistent with the Sverdrup relation that a uniform wind stress generates no currents in the final steady state (Anderson and Gill 1975). This comparison further demonstrates the different nature of the island circulation and basin circulation. In the island case, the initial Kelvin wave coastal currents on the eastern and western coasts, although in opposite directions, will never interact with each other because the long wave from the western coast will be blocked by the western boundary of the basin. As a result, there will be a net circulation around the island in the final equilibrium state.

3. Island circulation forced by local wind: Numerical experiments

Our theory is substantiated by a numerical experiment in a 1.5-layer, fully nonlinear, reduced-gravity model

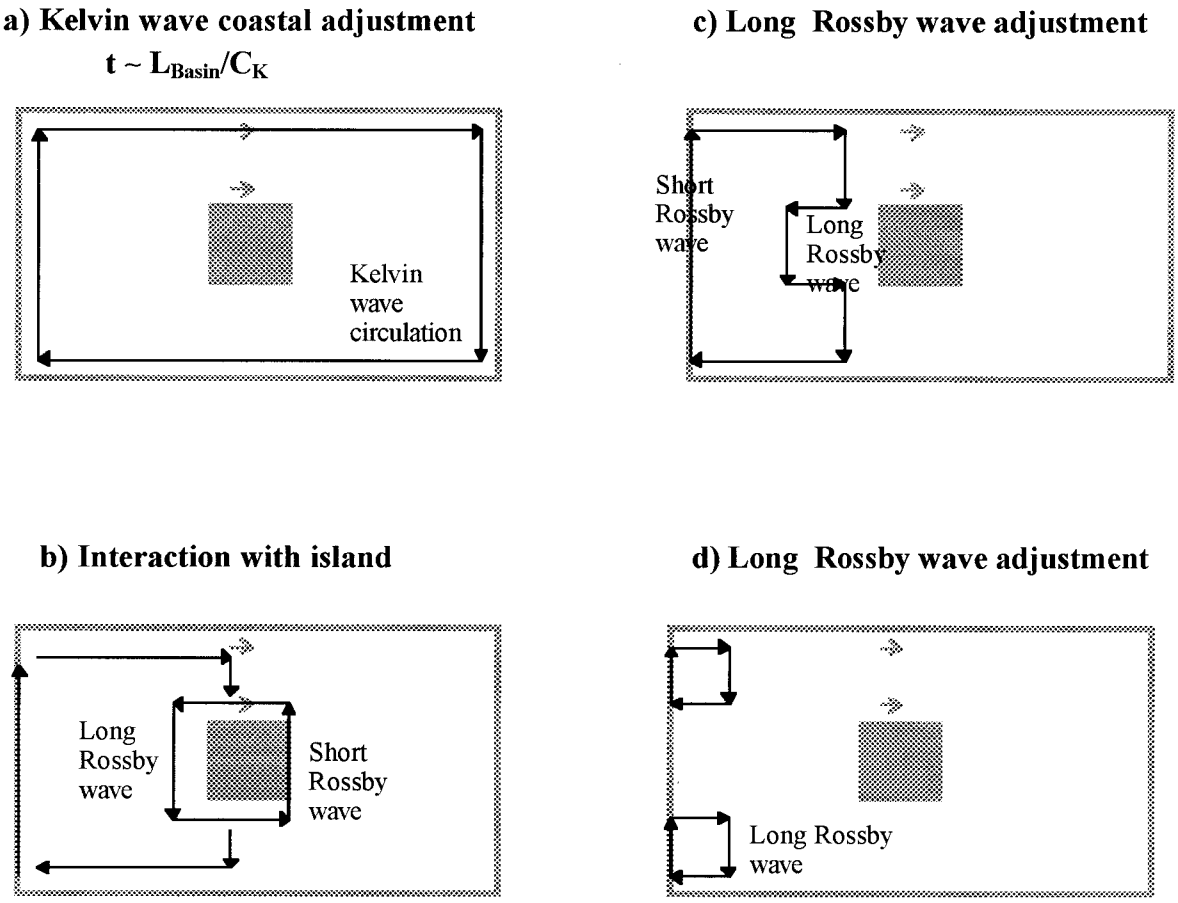

FIG. 3. Schematic figures for the formation of basin circulation spun up by an alongshore wind forcing. (a) Initial stage in which the counterclockwise Kelvin wave current is generated by the alongshore wind. (b) The second stage where short Rossby waves are generated along the western boundary of the basin, which balances the alongshore wind forcing and results in a northward western boundary current with an equilibrium transport that is determined by the island rule Eq. (2.1b). (c) and (d) The last stage in which the long Rossby wave generated by the primary Kelvin wave on the eastern boundary of the basin travels westward and interacts with the island, carrying with it a southward current. This long wave reaches the western boundary and cancels the northward boundary current, first in the middle part of the western boundary (d) and eventually along the entire boundary. Therefore, in spite of the similar first two stages of the spinup as in the island case in Fig. 2, the last stage differs dramatically between the two cases.

(Wallcraft 1991). The model is on a beta plane centered at $f_0 = 7.3 \times 10^{-5}$ s^{-1} ($y = 30°$N) with $\beta = 2 \times 10^{-11}$ m^{-1} s^{-1}. The model domain is (0°, 30°) × (20°N, 40°N) with 1° = 111 km, and the model resolution is ⅛°. An island is located at the center of the basin with zonal and meridional widths of 10° and 8°, respectively (see Fig. 4). A no-slip boundary condition is applied with the Laplace diffusion coefficient of 140 m^2 s^{-1}, corresponding to a Munk boundary layer width of about $\delta = 18$ km. The mean thickness is $D = 500$ m and the stratification is $\Delta\rho/\rho = 0.002$, corresponding to a deformation radius of 43 km in central latitudes. At the initial time $t = 0$, a zonal wind stress patch (with zero Ekman pumping) is imposed north of the island ($10° \le x \le 20°$, $34° N \le y \le 40°$N) with $\tau^x = \tau_0 y/y_1$, $\tau_0 = 0.1$ dyn cm^{-2} and $y_1 = 37°$N. This wind stress produces downwelling and upwelling Kelvin waves around the island and the basin boundary, respectively. Using the island rule (2.1) and the maximum amplitude (2.17b), the island circulation transport is 0.58 Sv (Sv ≡ 10^6 m^3 s^{-1}), and the maximum coastal SSH is $K_M = 0.95$ cm. Similarly, the basin boundary transport is 0.25 Sv and $K_M = 0.47$ cm.

Figures 4a–f plot six snapshots of SSH during the spinup process. The corresponding zonal and meridional SSH profiles are also plotted along the center latitude $y = 30°$N (Fig. 5a) and the center longitude $x = 20°$ (Fig. 5b) of the basin. The initial 15 days (Fig. 4a) is characterized by a positive SSH virtually uniform around the island, with an amplitude that has increased linearly to about 0.2 cm at the coast. The accompanied coastal Kelvin wave current, which is forced by the coastal downwelling on the northern edge of the island, circulates clockwise around the island and is trapped within about 50 km of the coast. This stage corresponds to the Kelvin wave coastal adjustment ($t_{\text{island}} \approx 13$ days in this case) as discussed in Fig. 2a.

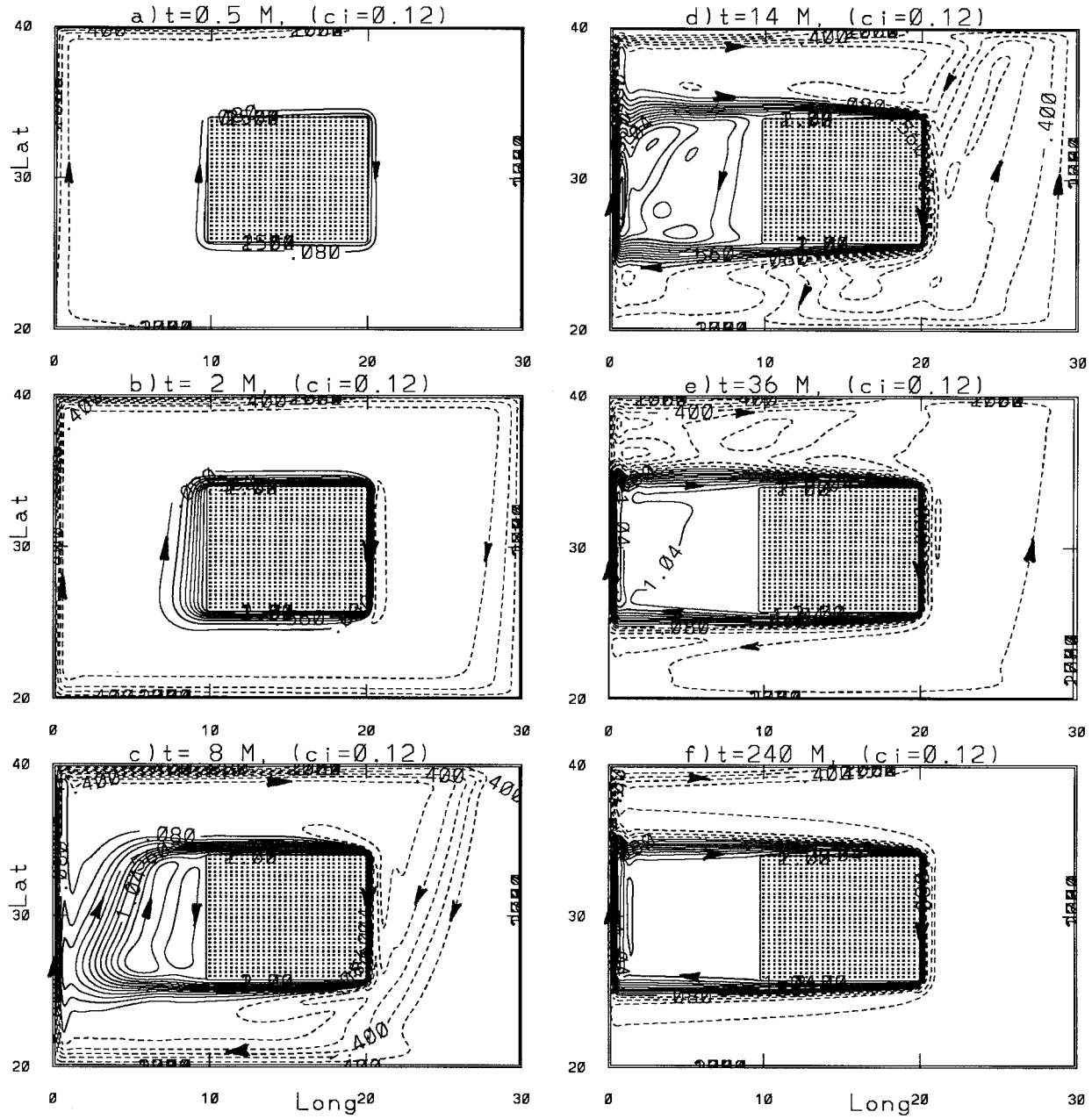

FIG. 4. Snapshots in a spinup process of island circulation in a 1.5-layer, beta-plane model experiment forced by the sudden onset of an alongshore wind stress north of the island (see the text): (a) t = 0.5 months, (b) t = 2 months, (c) t = 8 months, (d) t = 14 months, (e) t = 36 months, and (f) t = 240 months. Each snap shot is a 15 average with t being the end time. Contour interval is 0.12 cm.

The evolution of the transport in the initial 15 days can be seen in the time series in Fig. 6a along the northern, eastern, southern, and western boundaries of the island. The transports are roughly in phase on all the boundaries, although the maximum tends to occur first on the eastern, then southern, and finally the western and northern coasts. The magnitudes of transports are also roughly the same along all the coasts. Finally, the transport increases linearly with time, as discussed in (2.6), but has barely reached 0.1 Sv at day 15.

At day 15 (Fig. 4a, also Figs. 5a,b), a clockwise coastal Kelvin wave current is also generated on the basin boundary. This can be identified as the negative SSH tongue, which extends from the northern to the western boundary and finally diminishes along the southern boundary of the basin. Since the traveling time of the Kelvin wave around the basin is about 1 month, the coastal Kelvin wave current has propagated about half the circumference of the basin. The basin boundary Kelvin wave adjustment process that is discussed in Fig.

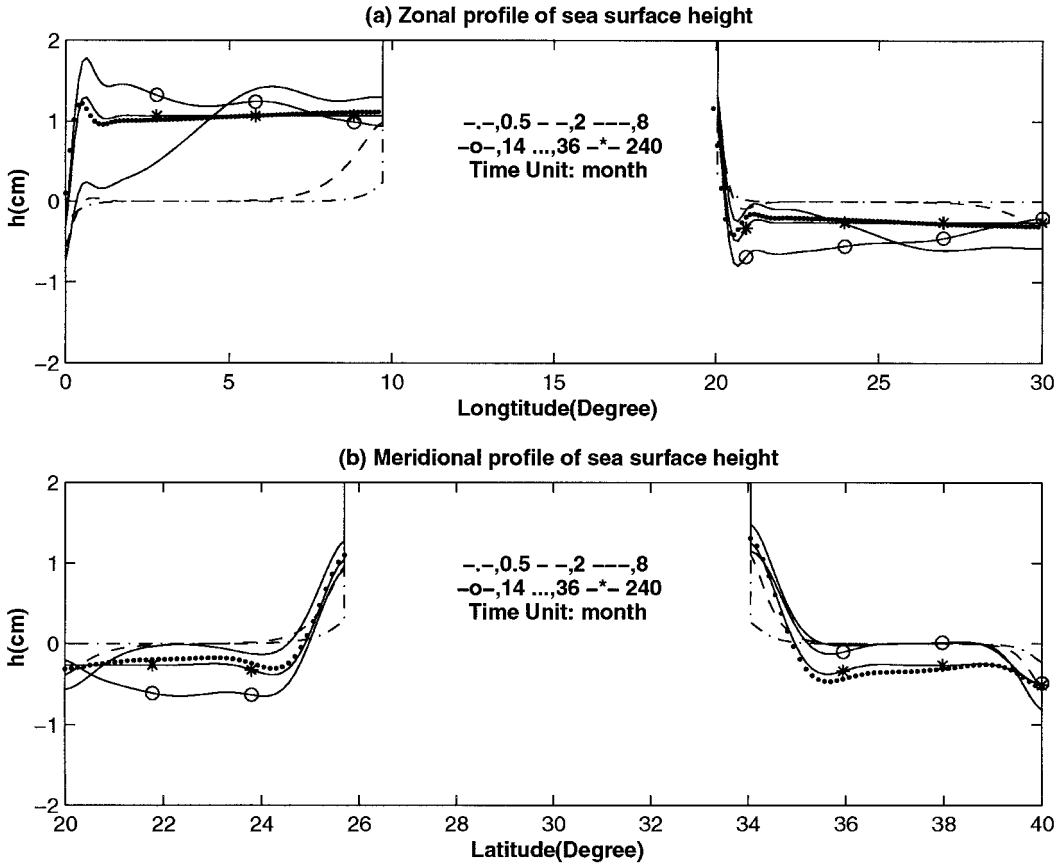

FIG. 5. The SSH profiles of the six snapshots in Fig. 4, along (a) the middle latitude $y = 30°$N and (b) the middle longitude $x = 15°$ of the basin. The line legends are dash–dot for $t = 0.5$ months, dash for $t = 2$ months, solid for $t = 8$ months, solid marked with circles for $t = 14$ months, dot for $t = 36$ months, and solid marked with stars for $t = 240$ months.

3a has not been completed yet. The alongshore transport of the basin boundary current also increases along all the basin boundaries (Fig. 6c), similar to the island circulation in Fig. 6a. However, the southern and the eastern boundaries tend to lag by about half a month due to the later arrival of the Kelvin wave. The coastal SSH and transport around the basin boundary are also smaller than those on the island boundary because of the larger circumference of the basin. This is consistent with Eq. (2.6).

Return to the island circulation. Figure 4b shows the SSH at the end of month 2 (which is after $t_{\text{damp}} \approx 1.5$ months in this case). The island circulation has increased significantly, with the coastal SSH and circulation transport reaching about 1 cm (Figs. 5a,b) and 0.5 Sv (Fig. 6a), respectively. The only exception is the west coast transport (Fig. 6a), which diminishes after 1.5 months because of the westward propagation of the long Rossby wave. Now, both the transport and coastal SSH are close to the theoretical equilibrium values according to the island rule (2.1b) (0.58 Sv.) and (2.17b) (0.95 cm), respectively. The boundary current (or SSH anomaly) is confined within a width of about 30 km along the eastern coast (Fig. 5a) due to the short Rossby waves, but they are spread over 100 km along the northern and southern boundaries due to the Kelvin wave (Fig. 5b) and over 200 km on the western coast (Fig. 5a) due to the propagating long Rossby wave. It is the narrow east coast boundary current that dominates the circulation and dissipation integral, and therefore determines the equilibrium transport. Indeed, the transport around the island remains close to its final value after about month 3 (Figs. 6a,b). This stage corresponds to the adjustment of short Rossby waves around the island, as discussed in Fig. 2b.

A similar short Rossby wave adjustment stage occurs along the western boundary of the basin after month 2 (Fig. 4b). The coastal SSH reaches about 0.5 cm (Figs. 4b and 5a,b), and the transport increases to 0.25 Sv except on the eastern boundary where the long Rossby wave has radiated away (Fig. 6c). Both the SSH and boundary transport are close to those estimated from (2.17b) (0.47 cm) and the island rule (2.1b) (0.25 Sv.). So far, the evolution of the boundary current transport is similar around the island and the basin, but with a

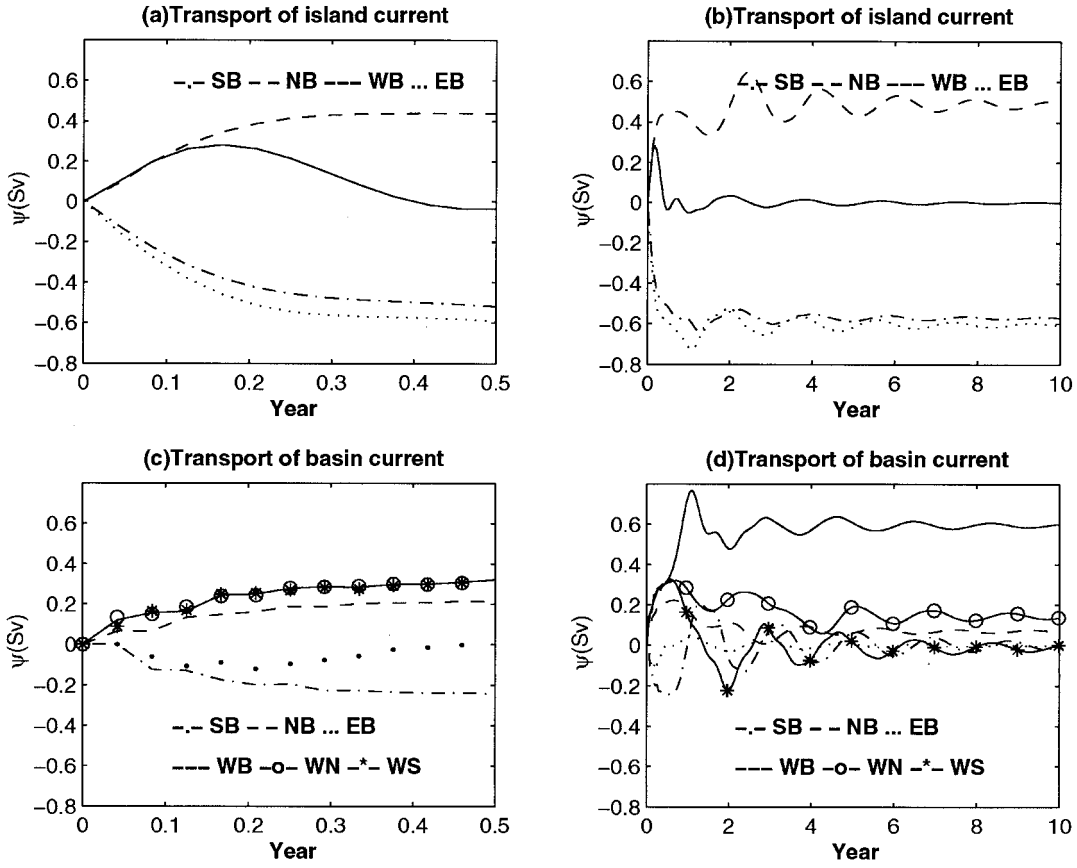

FIG. 6. The evolution of alongshore transports around the island: (a) first 0.5 year, (b) first 10 years, and around the basin: (c) first 0.5 year, (d) first 10 years. Each transport is calculated within 2° of the coast. For the island transports in (a) and (b), transports are plotted for cross sections in the middle of the eastern (dot, EB), southern (dash–dot, SB), western (solid, WB), and northern (dash, NB) coasts. For the basin boundary transports in (c) and (d), transports are also plotted for cross sections in the middle of the eastern (dot, EB), southern (dash–dot, SB), western (solid, WB), and northern (dash, NB) coasts. In addition, two additional transports are also plotted in the northern (y = 37°N, solid marked with circle, WN) and southern (y = 23°N, solid marked with star, WS) parts of the western boundary of the basin. In the first year [(c) or the initial stage of (d)], the three western boundary transport curves (WB, WN, and WS) almost coincide with each other, because the island effect has not reached the western boundary of the basin.

smaller transport because of the longer latitudinal extent of western boundary dissipation.

The following evolution of circulation is dominated by planetary wave propagation and its interaction with the boundaries of both the island and the basin. Eight months after the spinup (Figs. 4c and 5a), the long Rossby wave from the western coast of the island has almost reached the western boundary of the basin, while the long wave from the eastern boundary of the basin has almost reached the eastern coast of the island. The SSH fields on the northern and southern boundaries, however, remain virtually unchanged (Fig. 5b). The transports around the island and basin boundaries also remain close to that at month 2 (Figs. 6a–d).

After 14 months (Figs. 4d and 5a,b), the long wave from the western coast of the island has reached the western boundary of the basin. This incident long Rossby wave produces two responses. First, short Rossby waves are generated along the western boundary of the basin. The associated dissipation enables the spatial pattern of the island circulation to reach its final equilibrium as discussed in Fig. 2c. The southward transport of the island circulation on the eastern coast of the island is returned by a northward transport that is now arrested by the western boundary of the basin. This island transport dramatically increases the total transport of the basin western boundary current in the middle latitudes (within the island's latitudes) as seen in Fig. 6d (solid line in early year 2). Second, due to mass conservation, the positive long Rossby wave SSH produces a positive secondary Kelvin wave anomaly and an accompanying counterclockwise Kelvin wave current along the basin boundary (for more details, see Liu et al. 1999). This is plotted schematically in Fig. 2c as the dashed line with arrows. This secondary positive Kelvin wave cancels part of the old negative basin boundary Kelvin wave signal. The reduction is seen most clearly in the southeastern part of the basin (Fig. 4d) where the negative

anomaly due to the initial Kelvin wave has left. The resultant circulation southeast of the island becomes cyclonic.

In the mean time, the basin eastern boundary planetary wave front has interacted with the island. The interaction is similar to the interaction of the island induced planetary wave on the western boundary of the basin as discussed above. Due to mass conservation, the incidental negative SSH produces a Kelvin wave current with negative SSH and counterclockwise circulation around the island, as shown schematically in Fig. 3b. As a result, the previously positive SSH around the island is reduced, as seen most clearly in Fig. 5a. The prior clockwise circulation around the island is also reduced as seen most clearly in the transport (Fig. 6b) after year 1. A weak southward current also radiates westward as a new long Rossby wave from the west coast of the island as seen in Fig. 4d (and schematically in Fig. 3b). The current on the southern boundary of the island increases, with the additional transport recirculating cyclonically due to the long wave from the eastern boundary of the basin (Figs. 4d and 5b).

In the later stages of the evolution, the island circulation fluctuates around its final equilibrium (Fig. 6b) because of the transient adjustment of Rossby waves and Kelvin waves. The western boundary transport component that is caused by the basin boundary Kelvin wave diminishes, because of the arrival of the basin eastern boundary long wave at the western boundary as discussed in Figs. 3c and 3d. The evolution of the western boundary transport differs among the southern, middle, and northern sectors. The southern part of the western boundary transport diminishes first (at about year 1.5 as seen in the solid line marked with stars in Fig. 6d) because of the fast propagation of long waves at low latitudes. In the middle sector, the transport is first enhanced by the island transport to reach the maximum of 0.75 Sv at year 1.2 (Fig. 6d), which is about the sum of the island transport and the transient basin boundary Kelvin wave transport. This transport, however, decreases and returns to the island transport at about year 1.5 because of the diminishing basin boundary current. Note that, although the middle sector is located at higher latitudes than the southern sector and therefore has a slower long wave propagation from the east, the adjustment timing is comparable to the southern part. This occurs because the interaction with the island accelerates the planetary wave front in the middle sector, owing to the rapid transmission of Kelvin waves around the island (Figs. 3b and 4d). On the western boundary of the basin, the diminished boundary current in the southern part and the equilibrium returning branch of the island circulation in the middle part can be seen in the snapshot at the end of year 3 (Fig. 4e). In contrast, the transport in the northern sector diminishes very slowly (Figs. 4e and 6d) because of both the slow planetary wave speed and the lack of interaction with the island. Finally, all the basin boundary transport vanishes except in the middle sector of the western boundary, which forms the returning branch of the island circulation (Figs. 4f, 5, and 6). There is also a weak basin boundary current in the northwestern corner (about 0.6 Sv as seen in the solid line with circles in Fig. 6d). This residual basin boundary current may be related to the fact that the northern part of the planetary wave from the eastern boundary of the basin is extremely slow and therefore is dissipated heavily during its interaction with the island's northern boundary. Overall, the numerical experiment strongly supports the theory presented in the last section.

Our study suggests that the short Rossby wave determines the final island circulation transport, while the long Rossby wave cancels the basin boundary current at the final equilibrium stage. If no Rossby wave exists, what will be the final circulation? In the absence of the short Rossby wave, the transport of the Kelvin wave current, either around the island or the basin boundary, should increase virtually linearly as in Eq. (2.6) because of the lack of an effective dissipation to balance the input angular momentum from the wind. Furthermore, the lack of long Rossby waves ensures that the coastal current will be trapped along the coast forever. These speculations are confirmed in a shallow water experiment on an f plane (Fig. 7). The experiment setup is identical to that used in Fig. 4 except $\beta = 0$. Initially at year 1, two Kelvin wave currents circulate clockwise around the boundary of the island and basin but remain separated (Fig. 7a). Both currents intensify dramatically with time. Their inertia increases so dramatically that they overshoot each corner (Figs. 7b,c). The width of both boundary currents also increases and eventually the two currents merge (Fig. 7d). The transports (Fig. 8) show an almost linear increase, which, after 20 years, become more than 10 times larger than the beta-plane case in Fig. 6. Even after 40 years (not shown), the transports are still increasing almost linearly as in Eq. (2.6). Clearly, both currents are forced resonantly by the alongshore wind. The island circulation is stronger than that along the basin boundary because of the shorter circumference of the former as suggested by Eq. (2.6). This example demonstrates clearly the critical importance of Rossby waves in the formation of the circulation both around the island and in the basin.

4. Island circulation forced by remote forcing

The island circulation can also be forced remotely by wind curl or Ekman pumping to the east of the island, as shown in (2.1c). In our generalized QG system, the Sverdrup flow to the east of the island is

$$T_{\mathrm{Sv}}(y) = \frac{f}{\beta} \int_{X_e}^{X_{be}} w_E \, dx, \tag{4.1}$$

where w_E is the Ekman pumping velocity; X_e and X_{be} are the eastern boundary of the island and the basin, respectively, as in Fig. 1.

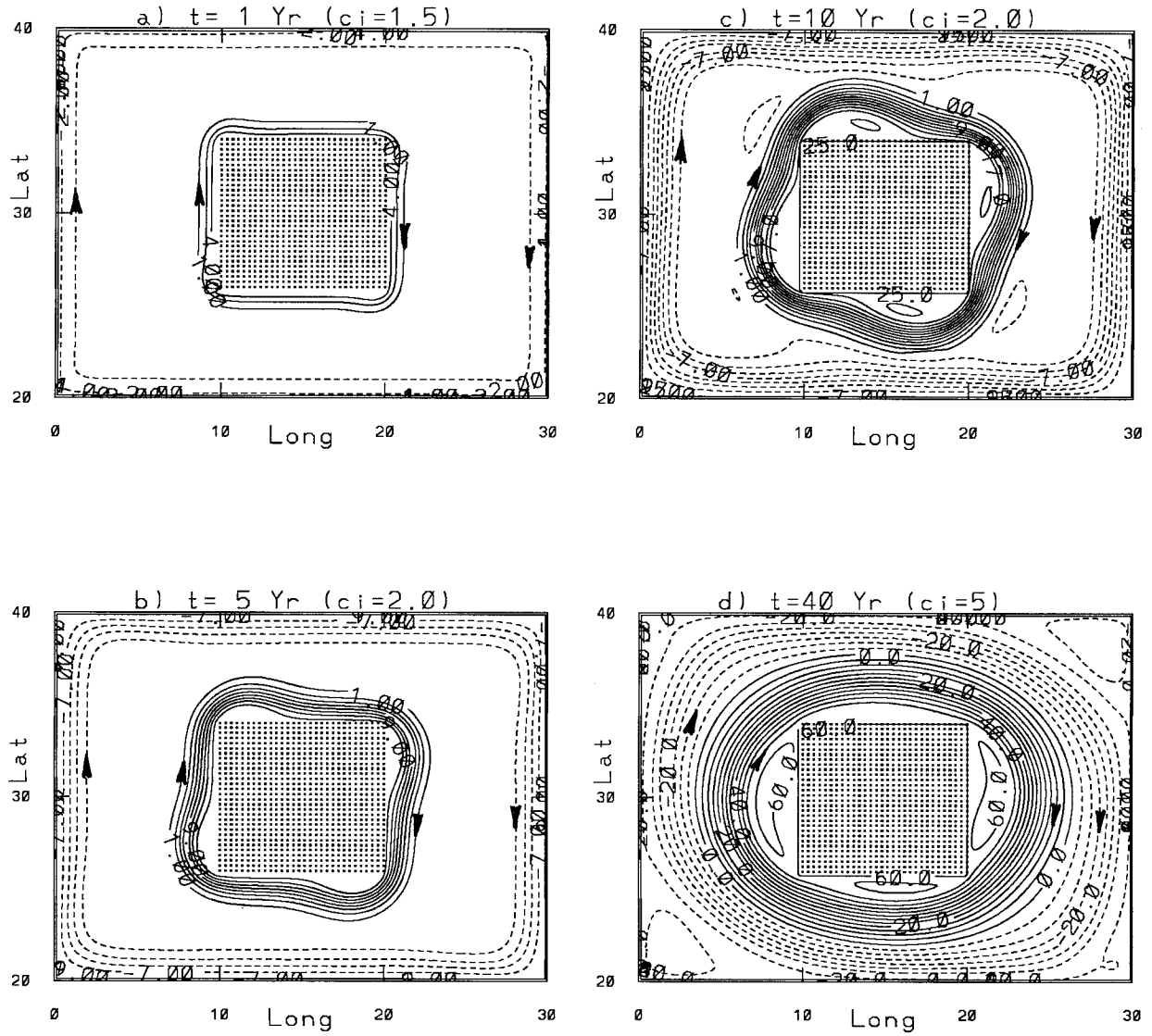

FIG. 7. Snapshots of SSH for a spinup experiment the same as Fig. 4 but on an f plane: (a) $t = 1$ year (contour interval = 1.5 cm), (b) $t = 5$ years (contour interval = 2 cm), (c) $t = 10$ years (contour interval = 2 cm), and (d) $t = 40$ years (contour interval = 5 cm).

Given a remote forcing, the spinup process of the island circulation is similar to the alongshore wind forcing case discussed before except that the Kelvin wave around the island is now initiated by the Sverdrup flow, which can be thought of as a steady long Rossby wave forced by Ekman forcing to the east of the island. After the onset of a steady Ekman pumping forcing (say, $w_E < 0$, as implied in Fig. 1), a long wave is established with a positive SSH and an anticyclonic circulation as shown schematically in Fig. 9a. This long wave reaches the eastern coast of the island, forming an interior Sverdrup flow with a southward geostrophic transport (Anderson and Gill 1975). In our generalized QG model Eq. (2.9), the SSH increase that occurs in the interior to balance the geostrophic contribution of the Sverdrup flow is

$$h_{RL}(x, y) = f \int_{X_{be}}^{x} w_E(x', y)\, dx'/g\beta D. \qquad (4.2)$$

This incident long wave on the eastern coast of the island generates short Rossby waves that are then damped quickly to form a northward returning boundary current. The boundary layer solution for the short Rossby wave can be derived from Eq. (2.9) as (Pedlosky 1987)

$$h_{RS}(x, y) = -h_{RL}(0, y)M(x), \qquad (4.3)$$

where h_{RL} corresponds to the Sverdrup flow SSH in Eq. (4.2) and $M(x)$ is the Munk boundary layer structure in Eq. (2.13). Most of the incident long wave energy is absorbed by the short Rossby wave (Pedlosky 1965).

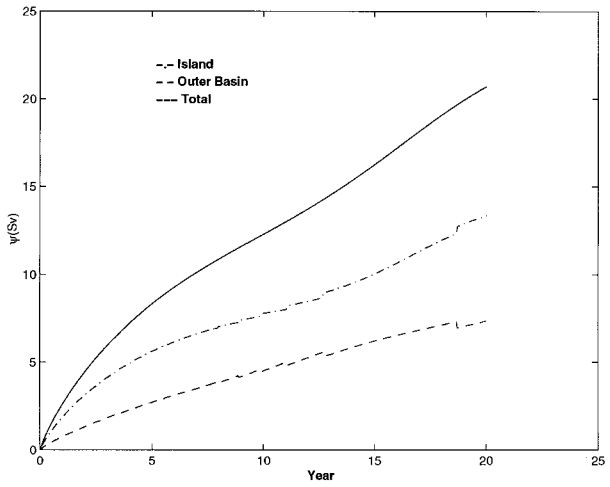

FIG. 8. Evolution of the total transport (solid), the island transport (dash–dot, calculated approximately as in the region of SSH > 0), and the basin boundary transport (dash, calculated approximately in the region of SSH < 0) for the f-plane spinup experiment in Fig. 7.

However, most of the incident mass leaks out through a coastal Kelvin wave [h_K, the same as Eq. (2.5)], which has a positive SSH and a clockwise current around the island (Liu et al. 1999). The following adjustment of the island circulation is similar to the alongshore wind forcing case discussed in section 2. This Kelvin wave generates short and long Rossby waves on the western and eastern coasts, respectively (Figs. 2b,c). The short Rossby wave (h_{KRS}) that is forced by the Kelvin wave is in the same direction as the Kelvin wave current and can be derived the same as Eq. (2.12) [also see Liu et al. (1999) and Godfrey (1975)]. Finally, the amplitude of the Kelvin wave $K(t)$ reaches its final equilibrium, which is accompanied by a clockwise island circulation (Fig. 2b). Later, the long Rossby wave to the west of the island propagates to the western boundary of the basin and the entire island circulation is established (Fig. 9c).

The final amplitude of the coastal Kelvin wave current can be obtained from the island boundary integral (2.3). In the absence of an alongshore wind $\Gamma_\tau = 0$, Eq. (2.3) requires that the total dissipation integral around the island vanishes at final equilibrium. Since the dissipation integral is contributed dominantly by the east coast of the island, we have

$$0 = \oint_{\text{island}} \nabla^2 \mathbf{u} \cdot d\mathbf{l}$$

$$\approx \int_{y_s}^{y_n} \partial_{xx} v|_{x=0}\, dy = (g/f) \int_{y_s}^{y_n} \partial_{xxx} h|_{x=0}\, dy. \quad (4.4)$$

In contrast to the case of alongshore wind forcing in Eq. (2.15), the eastern coast SSH consists of the Sverdrup flow, Eq. (4.2), and the returning boundary current, Eq. (4.3), as well as the primary Kelvin wave (h_K) in

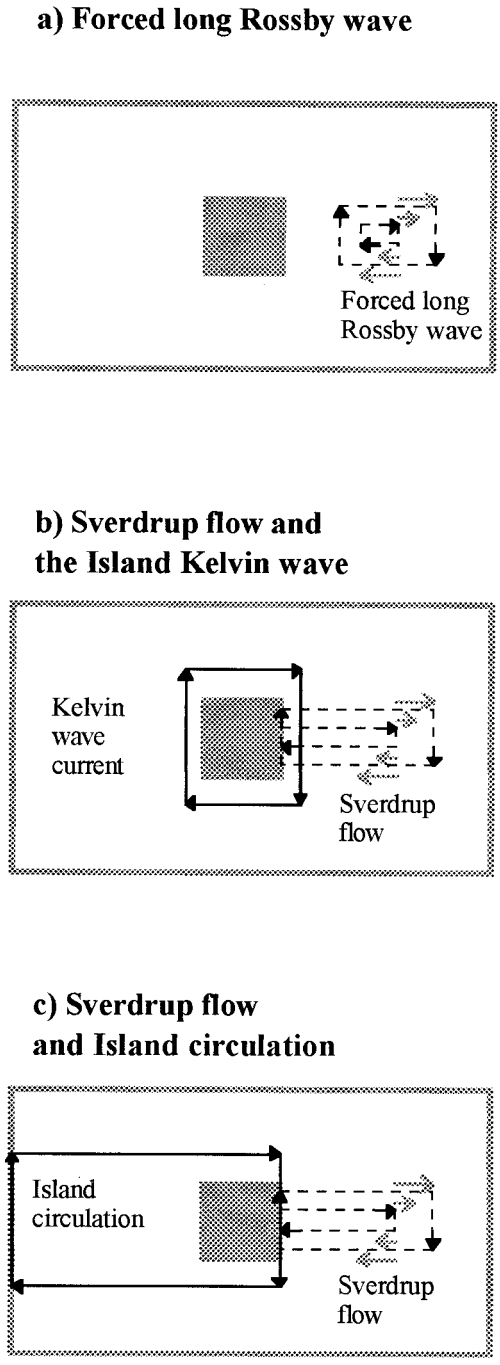

FIG. 9. Schematic figures showing the spinup of the island circulation (dark solid lines with arrow) by a remote anticyclonic wind curl forcing to the east of the island. (a) Ekman pumping forces a long Rossby wave (dashed lines with arrow). (b) The long wave propagates to the western boundary and the reflected short Rossby waves are arrested by dissipation to establish a northward returning boundary current on the eastern coast of the island, forming a gyre with the southward Sverdrup flow and a northward returning western boundary current (dashed lines). In the mean time, a Kelvin wave current is generated around the island (solid lines), which will generate an island circulation the same as in Figs. 2a–c. (c) The final circulation with the combined island circulation and the Sverdrup gyre.

Eq. (2.5) and the induced short Rossby wave (h_{KRS}) in Eq. (2.12); that is,

$$h = h_{RL} + h_{RS} + h_K + h_{KRS}.$$

The velocity dissipation along the eastern boundary of the island can be derived from (4.2), (4.3), (2.5), and (2.12). The contribution from the Sverdrup flow h_{RL} is negligible because of its large spatial scale. Therefore, at leading order,

$$\partial_{xxx}h|_{x=0} = [-h_{RL}(0, y) + K(t)]/\delta^3,$$

where the first and second terms are contributed by the returning boundary current h_{RS} and the Kelvin wave related current $h_K + h_{KRS}$, respectively. Therefore, the final amplitude K_m can be derived from Eq. (4.4) as the average SSH of the incident long wave (or Sverdrup flow):

$$K_m = \frac{\int_{y_s}^{y_n} h_{RL}(0, \tilde{y})\, d\tilde{y}}{y_n - y_s}. \tag{4.5}$$

This immediately recovers the island rule for a remote forcing in Eq. (2.1c).

The maximum coastal SSH amplitude, Eq. (4.5), is determined mainly by the balance of the contributions of two short Rossby waves, h_{RS} and h_{KRS}: the former is caused by the forced long wave (Sverdrup flow) and the later is induced by the Kelvin wave. Indeed, Eq. (4.5) can also be derived from a zero net circulation around the island:

$$\oint_{\text{island}} \mathbf{u} \cdot d\mathbf{l} = 0.$$

This can be understood as the conservation of island circulation in the absence of a local alongshore wind stress. Initially, the total island circulation is zero. When a long wave (h_{RL}) hits the eastern coast of the island with a positive SSH and a southward Sverdrup flow, a narrow northward boundary current (h_{RS}) is generated there. To maintain a net zero island circulation, a southward Kelvin wave current (h_K) is induced, which in turn generates a southward short Rossby wave current h_{KRS}. Since the Kelvin wave current (h_K) (and in turn the generated short Rossby wave h_{KRS}) is uniform along the coast, it needs to achieve the amplitude of the average boundary current of the Sverdrup flow as in Eq. (4.5). A by-product is that the island circulation is stronger than the returning western boundary current of the Sverdrup flow near the northern or southern tips of the island. As a result, a stagnation point is generated by the counterflows along the eastern coast, forming a recirculation, as discussed by Pedlosky (1994). The discussions in this section are also confirmed by numerical experiments (not shown). Similar numerical experiments have been performed by Pedlosky et al. (1997).

5. Discussions and summary

The formation of island circulation is investigated in light of the dynamics of coastal Kelvin waves and Rossby waves. An island circulation can be forced by either a local alongshore wind around the island or a remote forcing to the east of the island. The formation of the island circulation proceeds in three stages. First, the direction of the island circulation is initiated by a Kelvin wave current, which is generated either directly by a local alongshore wind or indirectly by a remotely forced long Rossby wave incident on the eastern coast of the island. In the mean time, the Kelvin wave generates short and long Rossby waves on the eastern and western coasts of the island, respectively. The short Rossby wave is damped on the eastern coast and therefore allows the island circulation to quickly reach a steady transport that is estimated from the island rule. Under a local wind forcing, the damped short Rossby wave balances the alongshore wind forcing; for a remote forcing, the short Rossby wave current forced by the Kelvin wave tends to balance that produced by the Sverdrup flow. Finally, the spatial pattern of the island circulation is completed after the long Rossby wave propagates from the western coast of the island to the western boundary of the basin. The island circulation therefore consists of a boundary current along the eastern coast of the island and a returning flow on the western coast of the basin, which are connected by two zonal jets.

Our spinup study also has important implications for the understanding of the temporal response of the island circulation to a low-frequency variable wind forcing. As discussed in section 2, the island transport as determined by the island rule is achieved after forcing in a short boundary layer momentum dissipation timescale t_{damp}. This damping timescale is usually less than a few months for both a barotropic flow or an upper-ocean total baroclinic flow. Therefore the variation seen in the island transport in response to a local wind forcing should follow the island rule, Eq. (2.1b), for a variable wind of annual, or even higher, frequency for both the barotropic flow and the total upper-ocean baroclinic flow. This seems to be the case of Masumoto and Yamagata (1996), who showed that seasonal winds along Australia's south coast generate seasonal variations in the Indonesian Throughflow. The situation is very different under a remote forcing because of the different response times of the Sverdrup flow (or long waves) of the barotropic and baroclinic flows. For a barotropic flow, the Sverdrup flow responds to the wind in weeks, and therefore the completion time for the formation of the island circulation lasts no longer than a few months. Thus, the island rule (2.1c) is still valid for winds of frequency lower than annual frequency (Wajsowicz 1993a; Qiu et al. 1999). However, for the upper-ocean baroclinic flow, the Sverdrup flow responds to the Ekman pumping in years, and therefore the island rule Eq. (4.1) will no longer be valid (Qiu et al. 1999) unless

the wind variation is slower than the basin transient time of the baroclinic wave.

Our study also implies that the response of the vertical structure of the island circulation to remote forcing could be controlled by complex processes. The responses are different between the barotropic and the total upper-ocean flow, which are controlled by the barotropic and first baroclinic modes, respectively. The long barotropic Rossby wave propagates westward because it is much faster than the mean flow, while the first baroclinic mode propagates westward because of the non-Doppler-shift effect (e.g., Killworth et al. 1997; Liu 1998, 1999). Therefore, the transport of the barotropic and upper-layer island circulation only respond to the remote wind to its east as shown in (2.1c). However, more complex vertical structure of the island circulation could be caused either by the surface wind and buoyancy forcing in the thermocline (Liu 1998, 1999), or by thermohaline mass forcing in the deep ocean (Kawase 1987; Pedlosky 1994). In the thermocline case, the vertical structure within the thermocline is controlled by second, or even higher, baroclinic modes, which in the interior ocean are strongly advected by the gyre circulation of the thermocline (Liu 1998, 1999). With nonlinear advection dominating, the flow could be controlled strongly by upstream source water (Nof 1996). Therefore, the vertical structure of the island circulation within the thermocline can be affected by the remote surface forcing upstream in the gyre circulation. For the deep ocean case, the island circulation can also originate from various deep water sources due to complex thermohaline circulation (Shriver and Hurlburt 1997; Lu et al. 1998). These speculations remain to be studied in the future.

Acknowledgments. Comments from two reviewers were helpful in improving the paper. We thank one reviewer for bringing our attention to an earlier work of Godfrey. The editorial help from Ms. M. Kennedy is also greatly appreciated. This work is supported by the Young Investigator Program of ONR and the Physical Oceanography Program of NSF.

REFERENCES

Anderson, D. L. T., and A. E. Gill, 1975: Spin-up of a stratified ocean with applications to upwelling. *Deep-Sea Res.,* **22,** 583–596.

——, and P. D. Killworth, 1979: Non-linear propagation of long Rossby waves. *Deep-Sea Res.,* **26A,** 1033–1050.

Godfrey, J. S., 1975: On ocean spindown. I: A linear experiment. *J. Phys. Oceanogr.,* **5,** 399–409.

——, 1989: A Sverdrup model of the depth-integrated flow from the world ocean allowing for island circulations. *Geophys. Astrophys. Fluid Dyn.,* **45,** 89–112.

Hirst, A. C., and J. S. Godfrey, 1993: The role of the Indonesian Throughflow in a global ocean GCM. *J. Phys. Oceanogr.,* **23,** 1057–1086.

Kawase, M., 1987: Establishment of deep ocean circulation driven by deep-water production. *J. Phys. Oceanogr.,* **17,** 2294–2317.

Killworth, P. D., D. B. Chelton, and R. A. de Szoeke, 1997: The speed of observed and theoretical long extratropical planetary waves. *J. Phys. Oceanogr.,* **27,** 1946–1966.

Liu, Z., 1998: Planetary wave modes in the thermocline: Non-Doppler-shift mode, advective mode and Green mode. *Quart. J. Roy. Meteor. Soc.,* in press.

——, 1999: Forced planetary wave response in a thermocline gyre. *J. Phys. Oceanogr.,* **29,** 1036–1055.

——, L. Wu, and E. Bayler, 1999: Rossby wave—coastal Kelvin wave interaction in the extratropics. Part I: Low frequency adjustment in a closed basin. *J. Phys. Oceanogr.,* **29,** 2382–2404.

Lu, P., J. P. McCreary, and B. A. Klinger, 1998: Meridional circulation cells and the source waters of the Pacific equatorial undercurrent. *J. Phys. Oceanogr.,* **28,** 62–84.

Masumoto, Y., and T. Yamagata, 1996: Seasonal variations of the Indonesian Throughflow in a general ocean circulation model. *J. Geophys. Res.,* **101,** 12 287–12 293.

McCalpin, J. D., 1995: Rossby wave generation by poleward propagating Kelvin waves: The midlatitude quasi-geostrophic approximation. *J. Phys. Oceanogr.,* **25,** 1415–1425.

Miles, J. W., 1972: Kelvin waves on oceanic boundaries. *J. Fluid Mech.,* **55,** 113–127.

Nof, D., 1996: What controls the origin of the Indonesian Throughflow? *J. Geophys. Res.,* **101,** 12 301–12 314.

Pedlosky, J., 1965: A note on the western intensification of the oceanic circulation. *Mar. Res.,* **23,** 207–1210.

——, 1987: *Geophysical Fluid Dynamics.* Springer-Verlag, 710 pp.

——, 1994: Ridges and recirculations: Gaps and jets. *J. Phys. Oceanogr.,* **24,** 2703–2707.

——, and M. A. Spall, 1999: Rossby normal modes in basins with barriers. *J. Phys. Oceanogr.,* **29,** 2332–2349.

——, L. J. Pratt, M. A. Spall, and K. R. Helfrich, 1997: Circulation around islands and ridges. *J. Mar. Res.,* **55,** 1199–1251.

Qiu, B., D. Hoh, C. Lumkin, and P. Flament, 1997: On the existence and formation mechanism of the North Hawaiian Ridge Current. *J. Phys. Oceanogr.,* **27,** 431–444.

——, W. Miao, and E. Firing, 1999: Time-dependent island rule and its application to the time-varying North Hawaiian Ridge Current. *J. Phys. Oceanogr.,* in press.

Shriver, J. F., and H. E. Hurlburt, 1997: The contribution of the global thermohaline circulation to the Pacific to Indian Ocean throughflow via Indonesia. *J. Geophys. Res.,* **102,** 5491–5511.

Wajsowicz, R. C., 1993a: The circulation of the depth-integrated flow around an island with applications to the Indonesian Throughflow. *J. Phys. Oceanogr.,* **23,** 1470–1484.

——, 1993b: A simple model of the Indonesian Throughflow and its composition. *J. Phys. Oceanogr.,* **23,** 2684–2703.

——, 1996: Flow of a western boundary current through multiple straits: An electrical circuit analogy for the Indonesian Throughflow and archipelago. *J. Geophys. Res.,* **101,** 12 295–12 300.

Wallcraft, A. J., 1991: The navy layered ocean model users guide. NOARL Rep. 35, Stennis Space Center, MS, 21 pp.

Williams, G. P., 1985: Geostrophic regimes on a sphere and a beta plane. *J. Atmos. Sci.,* **42,** 1237–1243.